

Metal Oxide-based Nanoparticles for Environmental Remediation: Drawbacks and Opportunities

Victor Ruíz-Santoyo¹, Paloma Serrano-Díaz¹, Beatriz Adriana Andrade-Espinoza², Yaily Fernández-Arteaga¹, Ma. Concepción Arenas-Arrocena^{*1}

¹ Interdisciplinary Research Laboratory, Department of Nanostructures and Bionanomaterials, National School of Higher Studies, National Autonomous University of Mexico, Boulevard UNAM 2011, 37684, León Guanajuato, México

² Department of Biomedical Sciences, University Center of Tonalá, Guadalajara University, N. Periferico Oriente. 555, 45425, Tonalá, Jalisco, México

* Corresponding author, e-mail: carenas@enes.unam.mx

Received: 15 February 2024, Accepted: 06 June 2024, Published online: 11 July 2024

Abstract

The use of structured metal oxide-based nanoparticles for environmental proposals arises from the adverse impact of human industrial activities that threaten the fragile balance of the environment. These nanomaterials characterized by their chemical and mechanical stability, modifiable bandgap, remarkable textural features, and notable optoelectronic properties have an important role in removing pollutants from the environment. Metal oxide-based nanoparticles have demonstrated remarkable capabilities by removing pollutants such as herbicides, microplastics, dyes, pesticides, antibiotics, microbial organisms, and heavy metals. Additionally, these materials can be incorporated into sensing devices for real-time monitoring and identification of pollutants in air, water, and soil, facilitating environmental risk assessment and pollution control. Nevertheless, the successful implementation of semiconductor nanoparticles faces drawbacks and challenges, including scalability, cost-effectiveness, and potential environmental impacts, necessitating thorough consideration. Ongoing research and development efforts are crucial to further explore the potential of semiconductor nanoparticles for practical solutions. The anticipated growth in the use of these nanomaterials in various commercial applications foresees a more sustainable and environmentally friendly future. Thus, this document aims to present how nanoparticles with diverse forms and adjustable physicochemical properties are a tool to conserve the ecological balance.

Keywords

metal oxide, nanoparticles, semiconductor, environmental, remediation

1 Introduction

It is widely recognized that contemporary society confronts important challenges linked to the deterioration of the environment and the depletion of resources [1]. Effectively tackling these issues requires innovative and sustainable approaches that can reconcile economic development with the preservation of the environment [2]. In the realm of scientific knowledge and technological progress, metal oxide-based nanoparticles (NPs) are seen as a promising category of materials with the potential future to improve environmental remediation and protection [3]. They present themselves as formidable aid tool in confronting diverse environmental challenges due to their remarkable features as quantum confinement effects, and modifiable optical, electrical, and photocatalytic properties. Metal oxide-based nanoparticles showcase their capability to redefine

the trajectory of environmental remediation [4]. In this sense, metal oxide nanostructures like ZnO, TiO₂, WO₃, CuO, Fe₂O₃, SnO₂, V₂O₅, Fe₃O₄, ZrO₂, and MoO₃ have been designed and developed for their application as composites or individual in different areas of environmental sustainability such as water decontamination, air purification, contaminated soil remediation, and energy storage [5]. These nanostructures display a diversity of operational properties, clearly related to their crystalline structure, morphology, electronic arrangement, inherent defects, doping, and synthesis route, which govern their optical, electrical, physicochemical, and photocatalytic properties [6]. The structural variety of metal oxide nanostructures is given by the process parameters and the chemical and physical synthesis techniques [7]. However, it is key to consider that

the lack of comprehensive regulation and assessment of these nanomaterials could present a challenge for their real and practical application [8]. Furthermore, the rapid proliferation of nanomaterials without a clear understanding of their environmental impacts raises the need for comprehensive research and regulatory measures [9]. Therefore, this review aims to present the potential of metal oxide-based nanoparticles as a means to improve and safeguard the ecological balance without compromising environmental health for future generations.

2 Metal oxide semiconductor nanoparticles

Metal oxide-based nanoparticles are nanomaterials with dimensions at the nanoscale in the range between 1–100 nm and are classified into natural, incidental, and engineered or manufactured. These materials have unique electronic, optical, and chemical properties compared to their bulk counterparts [10]. Some common metal oxide nanomaterial morphologies are irregular spherical particles, quantum dots (QDs), wires, flowers, rods, cubes, ovoids, spheres, polyhedral, and sheets [11], which are frequently used to remove a wide gamma of inorganic and organic pollutants, Fig 1.

Metal oxide semiconductor are valence compounds with a prominent ionic bonding degree with positive metal and oxygen in -2 oxidation state and present metallic, ducting, or insulating features [12]. Their conduction band and valence band mainly contain metal (M) ns and oxygen 2p orbital, respectively [13]. The interaction between the metal and oxide orbitals generates a substantial disparity in the charge carrier transport. In general, the M ns orbitals are highly unlocalized, while the O 2p one is localized, which relies on a smaller effective mass for electrons (e^-) compared to holes (h^+) [14]. The electronic configuration of devices based on semiconductor nanoparticles is essential to understanding their electrical properties, for this reason, the ability to

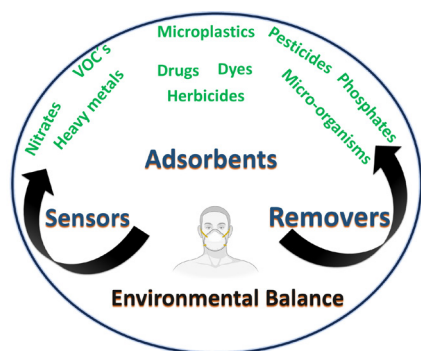


Fig. 1 Diverse applications of metal oxides nanoparticles for removal pollutants

control and manipulate the electronic configuration is essential to design devices with specific properties for electronic, and photonic applications [15]. The various nanoforms, synthesis methods, stoichiometric ratios, and used precursors give them properties to be used in environmental applications as shown in Table 1, 2 and 3 [16–51].

3 Metal oxide-based nanoparticles as photocatalysts for environmental remediation

Semiconductor nanoparticle photocatalysts transform renewable solar energy into electrochemical energy, utilizing light to excite electrons from the valence band (VB) to the conduction band (CD) in semiconductors with a bandgap close to or smaller than the incident light's energy [52]. This process creates free holes in the VB. Depending on the band edges' energy levels, these e^- s and h^+ s have the potential to interact with H_2O or O_2 molecules, leading to the formation of reactive oxygen species (ROS) like hydroxyl radical ($\cdot OH$) and superoxide radical ($O_2^{\cdot -}$) [53]. These ROS, in turn, can break down contaminant molecules until achieve the mineralization of them, i.e. their conversion to H_2O and CO_2 (Fig. 2). Simultaneously, the charge carriers can directly participate in reducing or oxidizing the target chemical species [1]. Consequently, through various chemical pathways, semiconductors have a crucial role in promoting environmentally friendly processes. Nevertheless, it is important to highlight that ROS production decreases as the charger carriers (e^- and h^+) suffer the recombination process by affecting their lifetime, thus inhibiting their operational photocatalytic performance [54]. To address the aforementioned problem, different strategies to improve photocatalytic performance as introducing point defects in semiconductors or forming heterostructures with other chemical compounds or periodic elements have been implemented [55]. The bonding of atoms has the potential to introduce extra energy levels between the valence and conduction bands, thereby improving light absorption through a reduction in the effective bandgap. Concurrently, the creation of a heterojunction between two diverse materials can expedite the efficient separation of charges, leading to an extended lifespan for charge carriers.

4 Nanoparticles for wastewater treatment

By 2050, about half of the world's population (57%) will be living in areas that experience water scarcity at least one month a year, hence, the shortage of water stands as a prominent challenge confronting nations in the contemporary world [56]. The rise in industrialization has resulted in the release of various pollutants, including heavy metals,

Table 1 Recent studies about photocatalytic removal of aqueous pollutants using metal oxide nanoparticles

Material	Synthesis route	Shape	Pollutant to remove	Experimental Conditions	Results	Ref.
QD immobilized MOF-5/ Ni-Co-layered double hydroxide (QD = Co, Ni, and Zn)	Via ultrasonication	Polyhedral-shaped	methylene blue (MB), rose Bengal (RB), and malachite green (MG) at 15 ppm.	8 mg added into 50 mL of solution (10 mg/L of MB and RB; 50 mg/L MG)	% removal of MB, RB, and MG was 96.2%, 95.8%, and 99.6%	[16]
ZnO/CeO ₂ /CeFeO ₃	Co-precipitation-calcination	Irregular	Tetracycline hydrochloride, amoxicillin, Congo red (CR), Fuchsin and Cr(VI) to Cr(III)	TCH (6.7 × 10 ⁻⁵ M), AMX (5.5 × 10 ⁻⁶ M), Fuchsin (7.7 × 10 ⁻⁶ M), and CR (1 × 10 ⁻⁵ M), and Cr(VI) (100 mg/L) using 100 mg of the powder	Removal values for ZnO/CeO ₂ / CeFeO ₃ and the reduction of Cr(VI) to Cr(III) were much higher than those for ZnO	[17]
Co-ZnO onto magnetic Fe ₃ O ₄	Co-precipitation	Irregular shapes and non-uniform size	MBTHC	1 g/L of powder was added to 100 ml of a solution containing 10 ppm of MB	MB (88.72%), while pristine ZnO (74.8%)	[18]
CeO ₂ nanorods	Hydrothermal synthesis with calcination	Rods in anisotropic growth	CR at 10 ppm	200 mL of CR solution at 20 ppm and 100 mg of CeO ₂	CR degradation of up to 97.7% in 130 min	[19]
NiTiO ₃ immobilized on glass	Spin-coating procedure	Rough surfaces and agglomerated (3.2 nm)	2,6-dichlorobenzamide (BAM) at 10 ppm	100 mL of BAM and 10 ppm, pH = 5.2	Sample with 1 wt% of Ni had a removal of 92.56% and sample with 2 wt% Ni had a 63.2% at 240 min	[20]
TiO ₂ /Reduced graphene oxide (rGO)	Hydrothermal/ solothermal	Crystalline agglomerates of spherical shape	MB	30 mL of solution at 10 mg/L	TiO ₂ /rGO 8 wt% had a removal % of 99.2% after 2 h under simulated solar light	[21]
Natural zeolite supported g-C ₃ N ₄ /ZnO/Ag ₃ PO ₄ sample	Precipitation and solid-state	Aggregates of particles with no defined shape.	Methyl orange (MO)	100 mL of MO solution and 0.15 g of powder at 24 °C	87.1% under optimized conditions	[22]
Cu ₃ (PO ₄) ₂ /MgO	Co-precipitation	Spherical/rods and plate-like structure (26-37 nm)	Amaranth dye	0.1 g/L, 10 μM of amaranth and 150 min	99% under solar irradiation using 0.1 g/L, 10 μM and 150 min of reaction	[23]
Mn ₃ O ₄ -ZnO	Chemical precipitation	No mentioned	MB	10 mg/L of MB, 10 mg of catalyst and 100 mL of dye	~98% removal of MB under UV-visible lamp	[24]
Graphite-TiO ₂ -doped coated sand granules	Polymeric	Graphite coat on the surface of the sand granules	MB	10 ppm	90% removal for 90 min	[25]
CuO-NiO-HNT (Halloysite nanotube)	Green approach via non-conventional microwave/ultrasonication	Nanotubular and cubic block like structure	CR	CR = 10 ppm, TC = 20 ppm and 30 mg of composite	In 90 min were reached 82% and 84% of degradation for CR and TC respectively	[26]
Calcium oxide nanoparticles	Biosynthesis method from golden linseed	Small clusters with different particle sizes.	Yellow tartrazine (YT) dye (20 mg/L)	YT=20 mg/L, CaO-NPs=1.2 g/L and pH = 7.0	76.2% of photodegradation	[27]
Doped sulfur over BiOBr	One-pot solvothermal approach	Microspheres with size of 1.0 μm, and consisted by layered nanosheets	Rhodamine B (RhB) and MB	15 mg/L RhB and 20 mg/L using 20 mg of catalyst in 40 mL of RhB (or MB) solution	RhB and MB degradation of 91% and 86% in 60 min under LED lamp	[28]

Table 2 Recent studies on the removal or sensing of air pollutants using metal oxide nanoparticles

Material	Synthesis route	Shape	Removed or sensed pollutant	Experimental conditions	Results	Ref.
Ag/SnO ₂	Photoreduction route	Rods with 10 nm of diameter and hundreds nm in length	NO	500 ppb of NO _x and 0.2 g of Ag/SnO ₂	NO removal of 50.6% at 30 min	[29]
Ce _{0.5} Mn _{0.3} Zr _{0.2} O ₂	Citrate method with chelating agent	Sponge-like structure	CO oxidation and soot combustion	Reaction mixture of 1 vol% CO, 5 vol% O ₂ , and 94 vol% He	Ce _{0.5} Mn _{0.3} Zr _{0.2} O ₂ material displayed a total CO conversion at 160 °C	[30]
WO ₃ /WS ₂	Hydrothermal synthesis and thermal annealing	Nanosheets and flakes (500 nm)	Sensitivity and selectivity to NO ₂	NO ₂ gas concentration varying from 2 to 10 ppm in a static gas sensing setup at room temperature	Response of 123% for 10 ppm NO ₂ with response/recovery time of 11 s/163 s at RT	[31]
Sn ₂ O ₃	Hydrothermal route	Nanorods with 400 and 80 nm in length and diameter	Sensing of acetone, ethanol, and formaldehyde	250 °C and from 1 to 400 ppm	Better sensitivity to Ac than others. At 250 °C the response R_{gas}/R_{air}^* to 1 ppm of Ac was 3.41 with 125 s and 43 s for response and recovery	[32]
(TiO ₂ , SnO ₂ , ZnO)/CNTs	Ball milling route	Fibers (10.2 to 13.5 nm) and spheres (20 – 30 nm)	NO _x removal	0.20 g of samples, 15 mL of NO (100 ppm) and humidity at 70%	SnO ₂ /CNTs, ZnO/CNTs, and TiO ₂ /CNTs samples showed 10%, 10.1%, and 41.25% degradations after 30 min. under visible light	[33]
Ag/Al ₂ O ₃	Impregnation and H ₂ treatment	Tin, single, and non-defined shapes (4.7 – 5.1 nm)	CO oxidation	Ag/Al ₂ O ₃ (10 mg) using a gas mixture of 0.4% CO, 10%O ₂ and balance Ar was fed at 50 mL/min	CO conversion (<30%) at 50 °C	[34]
Fe nanoparticles stabilized in carbon	Chemical vapor synthesis	Agglomerated particles of nano-Fe/C (< 8 nm)	Conversion of NOx	Gas mixture (0.9 mol% NO ₂ , 10 mol% Ar, 89.1 mol% He) at ambient pressure	Fe/C had higher NO _x -removal compared with untreated or iron-infiltrated activated C/Fe ₃ O ₄	[35]
CeO ₂ -loaded MnO ₂	Hydrothermal and adsorption-calcination technique	Flower-like morphology (200 – 300 nm)	Reduction of NO _x with NH ₃ at low temperatures	50 mg of powder and 200 mg of quartz sand with a flue gas mixture of NO (500 ppm), NH ₃ (500 ppm), O ₂ (2%), and balance gas N ₂	A complete NO _x conversion at 200 °C	[36]
Ag/SiO ₂ aerogel	Sol-gel followed by supercritical ethanol drying method	Ag spherical (15 – 20 nm)	Low temperature CO oxidation	20 mg of powder and the feed gas mixture was 100 mL/min, constituted of CO/O ₂ mixtures (3.6/20%) balanced with He	Maximum conversion (100%) at 290 °C	[37]
Au on rGO@Mg-BTC	Modified Hummers' method and solvothermal	2D nanosheets and spherical Au (14.6 – 15.9 nm)	CO oxidation	Gas mixture containing 76.0 wt% Ar, 20.0 wt% O ₂ , and 4.0 wt% CO with 0.7 g of the powder	100% CO conversion at 48 °C	[38]
Au-WO ₃ -NT titanate nanotubes (NTB)	Sol-gel and hydrothermal	Au between 1 – 3 nm and titanate size of 9 – 10 nm	CO oxidation	40mg of catalyst and the gas mixture (1 vol% CO and 1 vol% O ₂ balanced with N ₂) was introduced with a total flow rate of 100 mL/min	CO conversion of 97% at 20 °C	[39]
Fe ₂ O ₃ /Al ₂ O ₃	Chemical vapor deposition	Hemispheres of 700 μm	Low temperature CO oxidation	1% CO/air gas were tested using 2.0 g of catalyst at 450, 600, 750, and 900 °C	Fe ₂ O ₃ /Al ₂ O ₃ had 95% of activity at 100 °C	[40]

* R_{gas} : resistance in present of target gas, R_{air} : resistance in presence of air

Table 3 Metal oxide nanoparticle applications for the remediation of contaminated soil

Material	Synthesis route	NP Size (nm)	Pollutant to remove	Conditions	Results	Ref.
Zinc-iron layered double hydroxide	Nucleation and separate aging method	150	As(III)-contaminated water and soil	As(III) initial concentration of 200 mg/L with pH of 8.4	Adsorption capacity to As(III) was of 134.5 mg/g at 240 min. and was reduced the As concentration from 20 mg/L to a low level of smaller than 10 µg/L. oxidation of As(III) to As(V)	[41]
TiO ₂ on cadmium bioaccumulation in ramie	TiO ₂ were prepared via a sol-gel method	15 – 20	Cd-contaminated soils	Ramie was cultivated in soil spiked with 5 mg/kg Cd, with or without 500 mg/kg TiO ₂	The addition of 500 mg/kg TiO ₂ to soil increased Cd concentrations by 35% in roots, 75% in stems, and 278% in leaves in comparison to control plants with not nanoparticles	[42]
Compost assisted Fe ₃ O ₄ in spherical shape	Sol-gel	20 – 30	2-ethylhexyl phthalate (DEHP)	29 °C, 75% humidity, and pH 7.3	DEHP concentration of 10 mg/kg, retention time of 35 days, nanoparticles dose of 0.99 g/kg achieved a removal effectiveness of 91.6%	[43]
TiO ₂ nanoparticles	Green via with <i>Cyperus brevifolius</i> and <i>Paenibacillus sp</i>	17 – 29	Anthracene	100 µl of 500 mg/L anthracene solution, 100 µl bacterial isolate and 100 µl of biosynthesized TiO ₂ NPs at the concentrations of 150 mg/L	TiO ₂ NP's decreased the concentration of anthracene up to 21.3% in water test and 37.9% in the soil sample after 30 days	[44]
Fe ₃ O ₄ nanoparticles	Oxidation-precipitation	11 – 18	Polyaromatic hydrocarbon (PAH)-contaminated soil	H ₂ O ₂ concentration of 78 mM, Fe ₃ O ₄ NPs dosage of 18 mM, ultrasonic power of 313 W and pH 3.46	Using a Fe ₃ O ₄ nanoparticles dosage of 18 mM, ultrasonic power of 313 W and pH = 3.46, the pyrene removal was of 98.37%	[45]
TiO ₂ nanoparticles and <i>Brassica juncea L.</i>	Sol-gel	<25	Cd removal from soil	Cd concentration of 10 mg/kg and 100, 250, and 500 mg of TiO ₂ per kilogram of soil	Cd removal by TiO ₂ concentrations of 0, 100, 250, and 500 mg/kg treatment was 32.46%, 11.62%, 17.55%, and 55.11%, respectively	[46]
ZnO	Sol-gel	45.23	As and Pb	Contaminated soil with As (0.02 mg of dry soil) and Pb (0.2 mg/kg of dry soil) and ZnO was applied to the soil at 0.3 and 0.6 mg/kg	The permissible concentrations of Pb and As in soil are 400 and 22 mg/kg, respectively. Values reported in the soils for this study were 92 and 40 mg/kg of Pb, and As, respectively.	[47]
TiO ₂	Co-precipitation	30 – 100	Cd(II) in biological soil crusts (BSC)	Metal-ion concentrations between 5–200 mg/L and TiO ₂ concentration was set as 25 mg/L	Cd(II) removal effectiveness improved by 26.70% in comparison than that of pure BSC	[48]
Magnetic Fe ₃ O ₄	Co-precipitation	<1µm	Removal of Cd, Cr, Cu, Fe, Ni, Pb, and Zn	Pollutants concentrations were 10 ppm and Fe ₃ O ₄ NPs (0.5 g) were mixed with 250 ml of the wastewater sample (pH=2.3)	Heavy metal removal efficiency varied between 69.6 and 99.6% at pH=0.7	[49]
TiO ₂ (P25)	Sol-gel	(20 – 30 nm)	Diphenylarsinic acid (DPAA)	The solution had 1000 mg/L TiO ₂ and 20 mg/L DPAA at 25°C	82% removal within 3 h using a DPAA concentration of 20 mg/kg	[50]
CeO ₂	Hydrothermal	≈ 900	Pb in soil	As (≈100 mg/kg soil) or Pb (≈300 mg/kg soil) with CeO ₂ or TiO ₂ applied to soil at 500 mg/kg soil	CeO ₂ increased Pb phytoavailability two fold at the test at day 260. It was ascribed to CeO ₂ reducing soil pH and/or outcompeting Pb ²⁺ ions for sorption sites	[51]

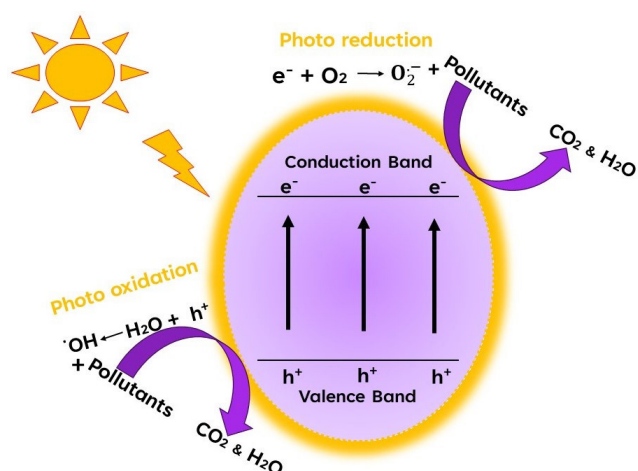


Fig. 2 Photo-generation of charge carriers in a semiconductor nanoparticle

drugs, pathogenic microorganisms, and endless chemical compounds derived from the manufacture of many consumables into rivers and streams, thereby endangering human health [57]. These pollutants must be eliminated before discharge through environmentally friendly treatment processes to reduce the environmental impact and the risks to human health that they pose [58]. Photocatalysis is widely used as a tool for the degradation and mineralization of organic molecules from wastewater. It has advantages over conventional processes as excellent oxidation ability, being environmentally friendly, and operating under standard temperature and pressure. The recent applications of characteristic metal oxide-based materials used as photocatalysts differentiated by various nanostructured shapes for wastewater treatment applications are shown in Table 1. In this context, Bhuyan et al. [16] studied the photodegradation under solar light of methylene blue (MB), rose bengal (RB), and malachite green (MG) through a metal organic framework (MOF) and a layered double hydroxide (LDH) modified with Co, Ni, and Zn quantum dots (MOF-5/Ni-Co-LDH) prepared by an ultrasound-assisted method. Samples had highly porous large polyhedral crystals shape. They found removal values for MB, RB, and MG were 96.2%, 95.8%, and 99.6%, respectively. Moreover, samples showed removal values of 85.6%, 89.3%, and 96.3% for MB, RB, and MG after 6 reaction cycles. Authors commented that the improved photocatalytic efficiency was ascribed to the enhanced light absorption capability by the QD deposited on the composite surface as shown in Fig. 3.

In another study, Andish-Lifshagerd et al. [17] investigated the degradation of tetracycline hydrochloride (THC), amoxicillin (AMX), Congo red (CR), Fuchsin and the reduction of Cr(VI) to Cr(III) using a ZnO/CeO₂/

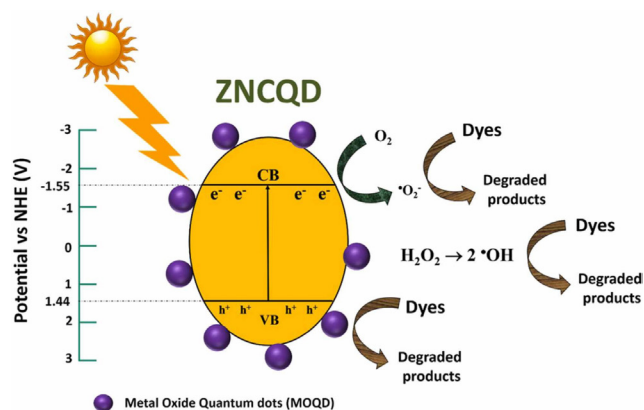


Fig. 3 Degradation way by MOF-5/Ni-Co-LDH under solar light [16]

CeFeO₃ photocatalyst driven under visible light prepared by a co-precipitation-calcination method. They found that removal values for ZnO/CeO₂/CeFeO₃ and the reduction of Cr(VI) to Cr(III) were much higher and faster values over the ZnO/CeO₂/CeFeO₃ photocatalyst than that of ZnO for the pollutants. Moreover, biocompatibility studies showed that photocatalytic treated wastewater was used for irrigating wheat seeds making them able to make it germinate efficiently. Finally, they concluded that the improved removals can be attributed to the differences in optical, electrochemical, and textural features, as well as to charge segregation related to the formation of n-n heterojunctions among ZnO, CeO₂, and CeFeO₃. On the other hand, Yik et al. [18] evaluated the photodegradation of MB using a Co-doped ZnO/Fe₂O₃ photocatalyst under visible light prepared via co-precipitation. According to the authors, the 5 mol% Co-ZnO (Co5-ZnO) sample with a band gap of 2.79 eV achieved the highest MB removal (88.7%) in comparison to that of ZnO (74.8%) with a band gap of 3.39 eV. The sample presented high agglomeration with variable shapes and non-uniform size. The authors demonstrated that (O₂^{·-}) had the most important role in pollutant removal due to the magnetic properties of the photocatalyst which was recovered using a magnet after photoreaction. Additionally, Rianjanu et al. [19] applied CeO₂ nanorods around 100 nm in diameter prepared using a hydrothermal route for the photocatalytic degradation of CR dye. Authors reported that at 2.16 h of reaction, removal of 97.7% of a CR solution at 10 ppm was achieved under UV light, as well as that (O₂^{·-}) and (h⁺) were responsible for the removal process, Fig. 4.

The authors concluded that the study provides a simple and effective route to prepare highly effective photocatalytic nanomaterials for dye removal. Recently, a visible-light-active NiTiO₃ coating developed by

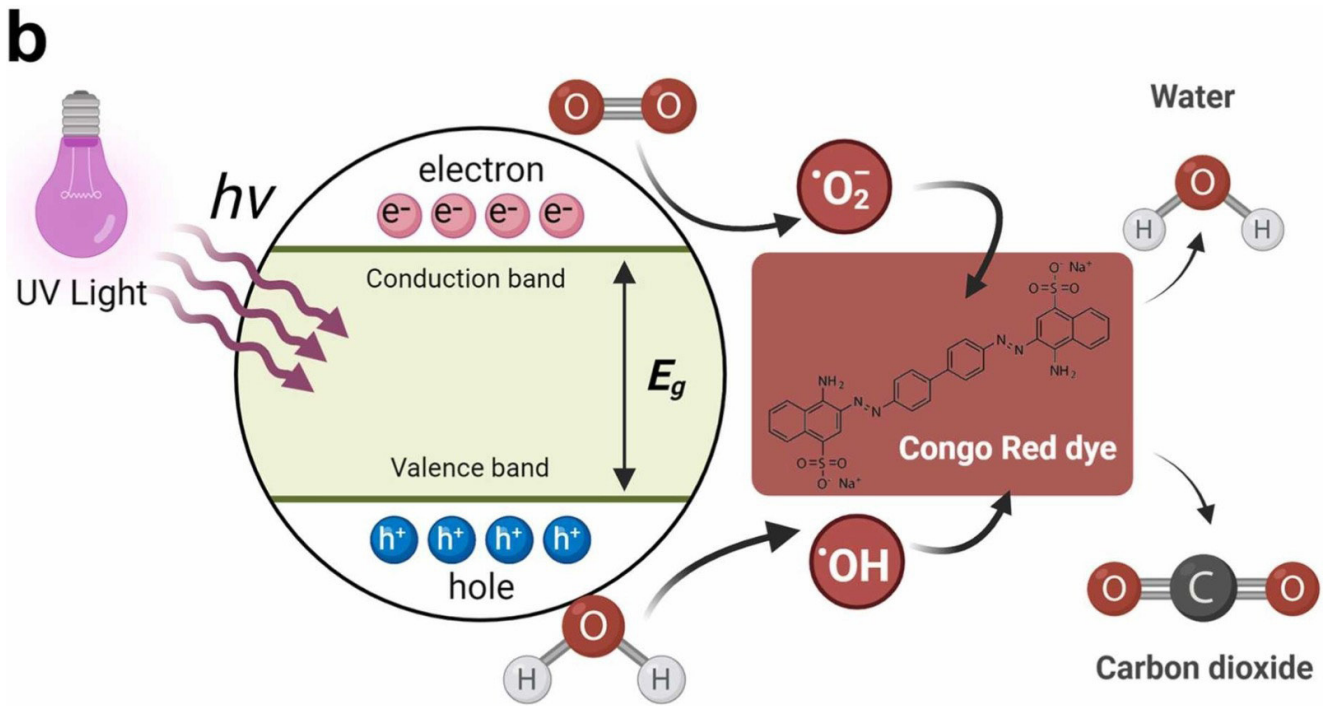


Fig. 4 Proposed degradation route for CR by CeO₂ sample [19]

Hernández-Del Castillo et al. [20] was prepared using a spin-coated method and studied for the removal of 2,6-dichlorobenzamide pesticide. The Ni wt% in NiTiO₃ were 1 wt% and 2 wt% and results showed that in 240 min of removal reaction, the sample with 1 wt% achieved a removal of 92.56% of the pesticide at 10 ppm, whereas the sample with 2 wt% of Ni achieved a 63.2%. Authors attributed the results to the BET area (159 m²/g), low band gap (2.4 eV), and physical stability of the samples, as well as the oxidative effect of the ·OH and O₂⁻ species, Fig 5.

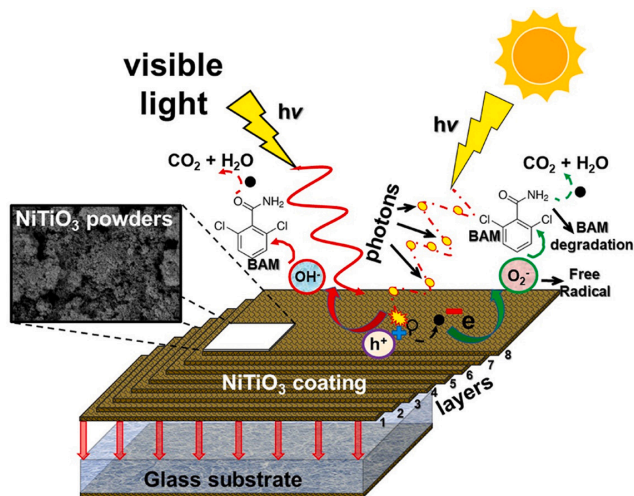


Fig. 5 Degradation of 2,6-dichlorobenzamide by NiTiO₃ [20]

5 Nanoparticles for gas sensing and air decontamination

Around the world almost 9 million of human being lose their lives annually due to air pollution, and 90% of the global population inhales air containing heightened levels of pollutants [59]. Adverse consequences on human health result from poor air quality, contributing to cardiovascular and visual diseases, asthma, allergic reactions, and cancer development [60]. Air pollution means alterations in the atmospheric composition due to the presence of biological, physical, or chemical substances emitted by biogenic, geogenic, or anthropogenic origins [6]. Those pollutants are classified as particulate or gaseous states that include aerosols of a biological nature, such as fungi, bacteria, and viruses, whereas gaseous form pertains to diverse chemical molecules such as volatile organic compounds (VOCs), NO_x and CO_x [61]. In this sense, Table 2 presents recent studies oriented to the elimination or sensing of air pollutants using metal oxide semiconductors. For example, Pham et al. [29] studied the NO removal under visible light using Ag nanoparticles onto SnO₂ nanorods prepared through a photoreduction route. Authors mentioned that the NO removal using the Ag/SnO₂ heterojunction achieved 50.6% after 30 min, almost twice higher than that of SnO₂ nanorods, with a lower NO₂ gas conversion

efficiency (1.0%), in comparison to that of SnO₂ (5.2%). The authors attributed the results to the photogenerated (h⁺) in the heterostructure, as shown in Fig. 6.

In another study, Grabchenko et al. [30] prepared via a facile citrate method different ternary CeO₂-ZrO₂-MnO_x samples with a sponge-like structure for studying the CO oxidation and soot combustion. In results, authors mentioned that the Ce_{0.5}Mn_{0.3}Zr_{0.2}O₂ material displayed a total CO conversion at 160 °C due to concentration of highly dispersed reducible MnO_x species, whereas the Ce_{0.5}Mn_{0.2}Zr_{0.3}O₂ material was more active at 490 °C in soot oxidation attributed to the creation of a great amount of interface boundaries between highly dispersed MnO_x species and Ce_{1-x}Zr_xO₂. The authors deduced that this study presents an approach for creating novel environmental catalysts exceptionally efficient. For their part, Patrick et al. [31] prepared WO₃/WS₂ materials using a hydrothermal route followed by a calcination process aimed at NO₂ gas sensing at room temperature, Fig 7.

Authors found that WS₂ nanosheets displayed a response of 26% towards 10 ppm of NO₂ with a response and recovery time of 13s/18s, while the WO₃/WS₂ sample annealed at 600 °C displayed a response of 123% with response and recovery time of 11s/163s. The authors mentioned that in the annealing treatment, the WS₂ had partial oxidation by creating WO₃ on the surface developing active heterojunctions

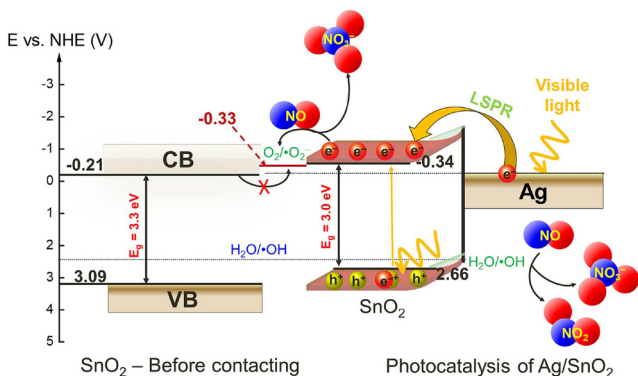


Fig. 6 NO gas decomposition by Ag/SnO₂ nanorods [29]

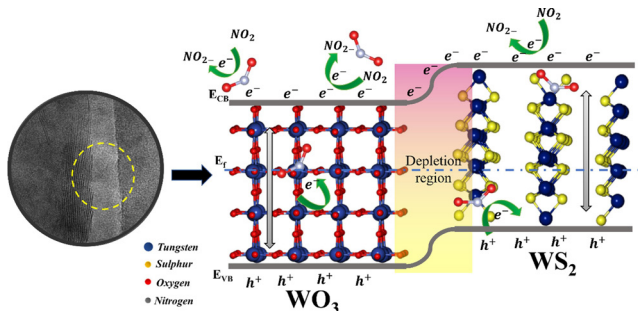


Fig. 7 Sensing structure of WO₃/WS₂ for NO₂ gas [31]

by incrementing the sensing performance. In another example, Samarium oxide (Sm₂O₃) nanorods with a single crystalline phase were prepared by Jamnani et al. [32] through a hydrothermal route to study their sensing properties acetone (C₃H₆O), ethanol and formaldehyde. The results showed that Sm₂O₃ nanorods achieved at 250 °C the resistance in presence of target gas/resistance in presence of air (R_{gas}/R_{air}) response to 1 ppm of acetone was 3.41 with a response and recovery times of 125 and 43 s, respectively (Fig. 8). Authors highlighted that Sm₂O₃ sensor is more active at low concentrations to C₃H₆O in comparison to CH₂O and C₂H₆O.

Recently, Nguyen et al. [33] studied the NO_x removal through SnO₂, ZnO, and TiO₂ mixed separately with commercial CNTs prepared by a ball-milling via. The best results including a high removal performance (42% at 30 min) the green products selectivity property (37% green products generation), and stability were achieved by the TiO₂/CNTs sample irradiated with visible light. In addition, the SnO₂/CNTs sample showed a high selectivity for the green products conversion, but a low total NO removal efficiency was reached. The authors concluded that the photogenerated h⁺ had a high influence as a key factor for NO photodegradation over TiO₂/CNTs. In another case of sensing gas, Pr doped In₂O₃ nanoparticles were synthesized using the co-precipitation method using a hydrothermal approach by An et al. [62] for ethanol gas-sensing performance. The results showed that the R_{air}/R_{gas} response of Pr-doped In₂O₃ (4% molar Pr/In) reached 112.4 at the ideal temperature of 140 °C, this response was 5.2 times higher than that of In₂O₃ material. Authors demonstrated that the Pr doping reduced the particle size of Pr/In₂O₃ composites as well as generated more active O₂ on the In₂O₃ surface by improving the Pr/In₂O₃-based sensors responses for C₂H₆O gas (112.40 – 50 ppm).

6 Nanoparticles for soil remediation

Soil is a limited resource, which means that its loss and deterioration are irreversible in the course of human life. The main reason behind the accelerated increase in soil erosion is attributed to human activity and associated land

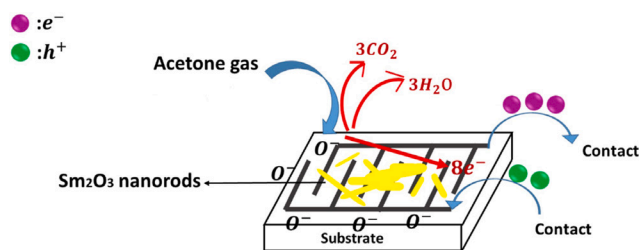


Fig. 8 Acetone sensing on Sm₂O₃ based conductometric device [32]

use changes due to as the population increases, more land is needed to produce food and raw materials [63]. This phenomenon has significant repercussions on nutrient and carbon cycling, soil desertification as well as on soil productivity, consequently affecting socioeconomic conditions at a global level [64]. For these reasons, different nanoparticles have been applied in the removal of soil pollutants by seeking their regeneration, Table 3. For example, Liu et al. [41] studied the synthesis and application of zinc-iron layered double hydroxide (ZnFe-LDH) prepared by nucleation and separate aging method to study its remediation performance to As(III) in water and soil under visible-light. Consequently, the adsorption capacity to As(III) reached 134.5 mg/g with less than 240 min and was reduced the As concentration from 20 mg/L to a low level of smaller than 10 µg/L. Moreover, the authors found that the transformation of As(III) to As(V) was related to the photooxidation via photogenerated h^+ , $\cdot OH$, and $O_2^{\cdot -}$. Fig. 9 (where NHE means normal hydrogen electrode) shows the photo-oxidation route of As(III) to As(V). They concluded that this approach of coupling photo-oxidation and adsorption improves the remediation performance of As(III)-polluted soil and water.

In another study, Deng et al. [42] studied the effects of TiO_2 nanoparticles on Cd bioaccumulation in ramie and its use in the remediation of cadmium-polluted soil. The TiO_2 was obtained via sol-gel method and presented a spherical shape with a size of 15 – 20 nm. The results proved that TiO_2 increased Cd concentrations by 35% in roots, 75% in stems, and 278% in leaves of ramie, in comparison to control plants. Moreover, with TiO_2 treatment, soil Cd levels

decreased by an estimated 20 – 30% after 2 months of ramie cultivation. This study shows the increased accumulation of Cd, particularly in the leaves by indicating the capability of TiO_2 to improve the phytoextraction effectiveness of ramie. Fe_3O_4 nanoparticles were applied in di(2-ethylhexyl)phthalate (DEHP)-contaminated soil remediation by Ghafghazi et al. [43]. In their study, the performance of kitchen organic waste compost assisted by Fe_3O_4 nanoparticles in DEHP removal using a DEHP concentration of 10 mg/kg, a retention time of 35 days, and a nanoparticle dose of 0.99 g/kg achieved a removal efficiency of 91.6 %. The authors concluded that the research showed an effective collaborative application of nanotechnology and biotechnology. In parallel Chakravarty et al. [44] studied the anthracene removal of polluted soil using *Alcaligenes faecalis* HP8 and TiO_2 nanoparticles prepared from *Paenibacillus* sp. HD1PAH and *Cyperus brevifolius*. The results showed that the application of TiO_2 and *Alcaligenes faecalis* HP8 decreased the anthracene concentration up to 21.3% in liquid at the end of 7 days and 37.9% in the soil treatments after completion of 30 days. Moreover, the suggested pathway for the degradation of anthracene augurs the three ring anthracene breakdown to one ring salicylic acid. In another case, Barzegar et al. [45] prepared Fe_3O_4 nanoparticles for the remediation of PAH-contaminated soil. The Fe_3O_4 was prepared using an oxidation-precipitation method and presented a particle size of around 11 – 18 nm. According to their results, using a Fe_3O_4 dosage of 18 mM, ultrasonic power of 313 W, and pH = 3.46, the achieved pyrene removal was 98.37%. The authors concluded that the findings revealed that removals ranged between 37.7% and 85.19% for other PAHs. These results were attributed to high pollution load, due to the presence of various and different PAHs and indicating a longer reaction time needed. For their part, Bakshi et al. [46] studied the possibility of using TiO_2 nanoparticles from Sigma Aldrich with *Brassica juncea* L., for exploring the removal of cadmium at 10 mg/kg to simulate a Cd-polluted soil. According to the results, Cd removal from the soil at TiO_2 nanoparticles concentrations of 0, 100, 250, and 500 mg/kg treatment were 32.46%, 11.62%, 17.55%, and 55.11%, respectively. Moreover, the translocations factor for Cd were 1.35, 0.96, 3.73, and 1.27 for 0, 100, 250, and 500 mg/kg concentrations, respectively. The findings of this research suggest that the utilization of TiO_2 nanoparticles in soil can alleviate Cd stress in plants and effectively extract it from the soil. Consequently, the integration of TiO_2 nanoparticles into the phytoremediation process holds promising

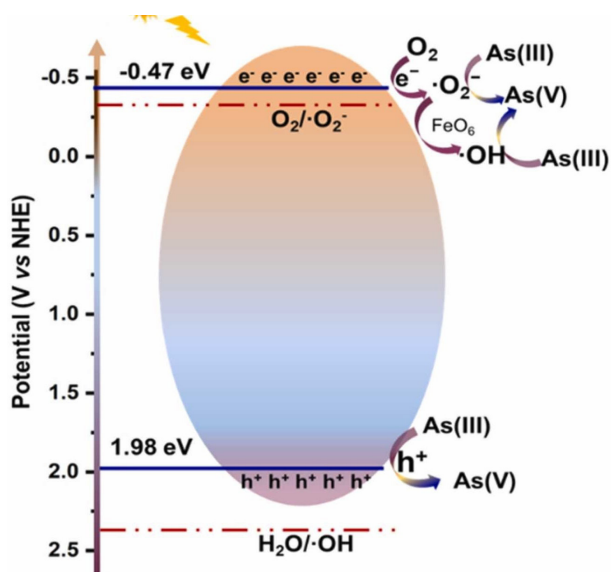


Fig. 9 Photocatalytic oxidation way of As(III) by ZnFe-LDH [39]

potential for addressing soil contamination issues. The authors proposed the interaction mechanism between TiO_2 and Cd removal as indicated in Fig 10.

Finally, Pérez-Hernández studied the performance of ZnO nanoparticles in sunflower plant growth (*Helianthus annuus L.*) for the removal of As and Pb from soils. In the study, was probed that ZnO at concentrations of 0.3 and 0.6 mg/kg dry soil enhanced the proportions of the plant and roots. Moreover, ZnO intensified the bioconcentration and translocation of As and Pb into the plant tissues as well. They concluded that the creep factor was higher than 1 at 25 and 45 days after plant emergence. Hence, the method of integrating phytoremediation with *H. annuus* and ZnO nanoparticles could present an innovative approach for cleansing soils tainted with As and Pb. In the described examples, the authors conclude, by pointing out that these studies are straightforward yet efficient approaches for creating potent materials designed for destroying pollutants, that subsequent research will concentrate on improving the material features towards the implementation of these materials on a larger scale. However, technical, scientific, and even environmental safety issues must first be resolved and some of these are discussed in Drawbacks and opportunities section.

7 Drawbacks and opportunities

As described in the paper, photocatalytic systems are seen as a supporting tool for the removal of emerging

contaminants in either wastewater treatment, air purification, or soil remediation. Dozens of research are published annually reporting designs and studies of nanostructures that remove contaminant molecules, however, most are experimentally idealized models. The question why these nanomaterials have not been taken to intensive way processes still remains and some proposed possible technical and scientific aspects could be: *i)* a longer contact time reaction between the pollutant molecule and its by-products with the generated ROS ($\cdot\text{OH}$ and $\text{O}_2^{\cdot-}$) because their half-life is nanoseconds and their production decreases with time and reuse cycles, *ii)* the advancement of characterization methods and tools for clarifying and verifying the routes taken by e^- and h^+ pairs in heterojunction photocatalysts, *iii)* incomplete mineralization of target molecule in aqueous medium due to the recombination rate of e^- and h^+ pairs, *iv)* the efficient design and operation of photocatalytic reactors is complex and requires careful control of parameters such as catalyst concentration, water flow rate and constant light intensity, *v)* the mass production of photocatalysts from affordable reagents is a must in order to operate under a favorable cost-benefit regime, *vi)* photocatalysis should be used as a final step in a decontamination process, not as a competing process to conventional ones, *vii)* the design of immobilized photocatalysts in continuous flux reactors should be further studied due to photocatalyst in powder involves its recovery at some point for reactivation (batch reactor) by

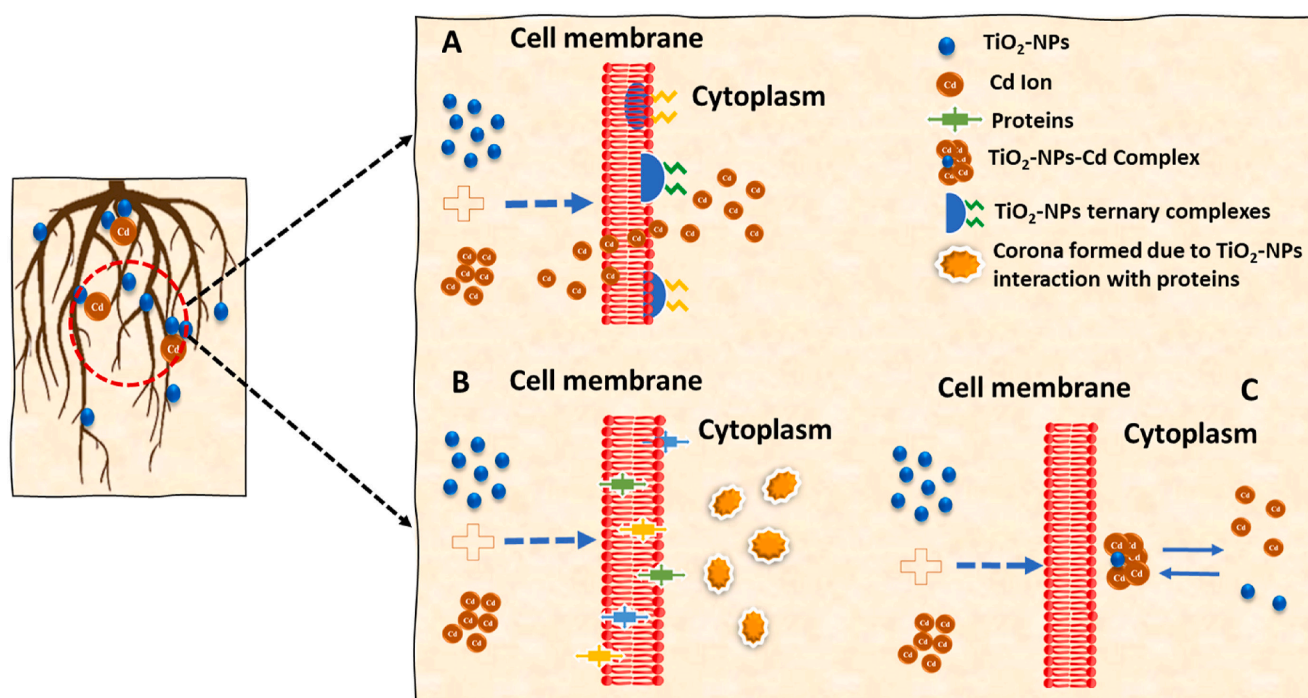


Fig. 10 Proposed interaction mechanism between TiO_2 and Cd [46]

increasing the operating costs, *viii*) the operation of photoactive photocatalysts operating under solar radiation to make the process sustainable despite adverse environmental operating conditions and, finally *ix*) aspects such as stability, selectivity, biodegradability, eco-friendly, recyclability, and cost-effectiveness (Fig 11). In soil remediation, through engaging with simultaneous pollutants in soil, nanomaterials could introduce an extra influence on the soil ecosystem, leading to combined toxicity of soil microbiome, varied bioaccumulation patterns, and complex overall effects. It has been proven that nano TiO₂ has claimed to increase the ecotoxicity or bioaccumulation of pollutants to animals and plants at cell the level by contributing to the imbalance of microorganisms in the soil and polluting the groundwater.

On the other hand, in future investigations, it is essential to focus on advancing sophisticated methodologies to evaluate nanomaterials across diverse environmental conditions. This will contribute to the progress in characterizing these elements at the nanometer scale. Such efforts will improve our understanding of their behavior, interactions, and potential risks, ultimately aiding in the creation of better effective mitigation strategies. An integral aspect of this pursuit involves interdisciplinary collaboration, requiring active engagement from scientists, policymakers, and environmentalists. Collaborative research groups with interdisciplinary expertise have the faculty to offer a comprehensive perspective on the phenomenon of pollution. In the journey to address pollution, the incorporation of scientific invention, policy expertise, and societal cooperation has the talent to shape the coming days where the hostile impacts of pollution are decreased, fostering a thriving environment characterized by balanced coexistence. Once the intensive and technique application

of nanostructures for remediation purposes has been resolved, it is important to consider that despite all possible benefits, it is critical to address concerns related to environmental safety and the potential toxicity of nanomaterials. A thorough assessment of potential risks is required before large-scale implementation. For example, some health agencies have warned of the toxicity of certain nanomaterials such as TiO₂ as potentially carcinogenic agents [65]. In this sense, public perception of nanotechnology in environmental remediation may influence its acceptance. Addressing concerns, providing transparent information, and engaging the public in discussions about the benefits and risks are important for fostering acceptance. Moreover, the regulatory framework for nanotechnology in environmental remediation is still evolving by establishing clear guidelines and regulations to ensure the safe and responsible use of nanomaterials. Addressing ethical concerns related to the potential unintended consequences is key also. Therefore, we must correctly choose the solution without collateral damage. Finally, the use of nanomaterials in environmental remediation is a promising and careful approach to addressing pollution challenges, offering efficient and sustainable solutions to preserve and restore the environmental balance.

8 Conclusion

Emerging pollutants, originating from substances like pharmaceuticals, personal care products, microplastics, consumable production byproducts, combustion gases, organic waste, fertilizers, and herbicides, pose a significant threat to both human health and the ecological balance of ecosystems. The application of nanomaterials in environmental remediation is a significant advance in the search for sustainable solutions to address environmental pollution. Nanomaterials with specific properties such as target specificity and a high specific surface area allow for greater interaction with contaminants present in the environment. This facilitates the efficient adsorption and capture of contaminant compounds by contributing to the purification of ecosystems. Furthermore, nanomaterial engineering facilitates functionalization to enhance the selectivity in capturing specific contaminants, thereby bolstering the efficacy of remediation processes. Nonetheless, while hybrid decontamination systems exhibit superior performance compared to individual methods, they pose challenges in terms of time, energy consumption, and cost. To tackle these challenges, nanostructures emerge as a promising solution. By leveraging these structures in monitoring

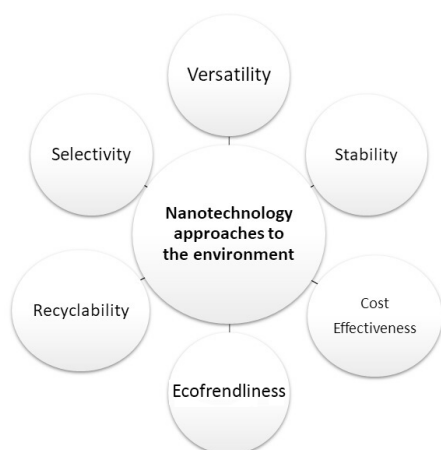


Fig. 11 Main nanotechnological and environmental approaches

applications, their adaptable and controllable properties can be optimized for maximum efficacy. Manipulating the properties of metal oxide nanoparticles holds substantial potential for significant advancements. This ongoing progress is driving the development of devices with heightened performance, transitioning from mere prototypes to practical, everyday applications by trying to ensure their industrial viability and economic feasibility.

References

- [1] Ruiz-Santoyo, V., Andrade-Espinoza, D. A., Romero-Toledo, R., Anaya-Esparza, L. M., Villagrán, Z., Guerra-Contreras, A. "Use of Nanostructured Photocatalysts for Dye Degradation: A Review", *Periodica Polytechnica Chemical Engineering*, 66(3), pp. 367–393, 2022.
<https://doi.org/10.3311/PPCh.18885>
- [2] Mishra, S., Sundaram, B. "A review of the photocatalysis process used for wastewater treatment", *Materials Today: Proceedings*, 2023.
<https://doi.org/10.1016/j.matpr.2023.07.147>
- [3] Kamali, M., Dewil, R., Appels, L., Aminabhavi, T. M. "Nanostructured materials via green sonochemical routes – Sustainability aspects", *Chemosphere*, 276, 130146, 2021.
<https://doi.org/10.1016/j.chemosphere.2021.130146>
- [4] Hairom, N. H. H., Soon, C. F., Mohamed, R. M. S. R., Morsin, M., Zainal, N., Nayan, N., Zulkifli, C. Z., Harun, N. H. "A review of nanotechnological applications to detect and control surface water pollution", *Environmental Technology and Innovation*, 24, 102032, 2021.
<https://doi.org/10.1016/j.eti.2021.102032>
- [5] Shahcheraghi, N., Golchin, H., Sadri, Z., Tabari, Y., Borhanifar, F., Makani, S. "Nano-biotechnology, an applicable approach for sustainable future", *3 Biotech*, 12(3), 65, 2022.
<https://doi.org/10.1007/s13205-021-03108-9>
- [6] Saleem, H., Zaidi, S. J., Ismail, A. F., Goh, P. S. "Advances of nanomaterials for air pollution remediation their impacts on the environment", *Chemosphere*, 287, 132083, 2022.
<https://doi.org/10.1016/j.chemosphere.2021.132083>
- [7] Parashar, M., Shukla, V. K., Singh, R. "Metal oxides nanoparticles via sol–gel method: a review on synthesis, characterization and applications", *Journal of Materials Science: Materials in Electronics*, 31(5), pp. 3729–3749, 2020.
<https://doi.org/10.1007/s10854-020-02994-8>
- [8] Sharma, R., Watanabe, T., Kumar, A. "Estimation of risk to soil and human health during irrigation using ZnO nanoparticles-containing water", *Journal of Environmental Chemical Engineering*, 11(6), 111230, 2023.
<https://doi.org/10.1016/j.jece.2023.111230>
- [9] Gayathiri, E., Prakash, P., Pandiaraj, S., Ramasubburayan, R., Gaur, A., Sekar, M., Viswanathan, D., Govindasamy, R. "Investigating the ecological implications of nanomaterials: Unveiling plants' notable responses to nano-pollution", *Plant Physiology and Biochemistry*, 206, 108261, 2023.
<https://doi.org/10.1016/j.plaphy.2023.108261>
- [10] Fu, P. P., Xia, Q., Hwang, M. H., Ray, P. C., Yu, H. "Mechanisms of nanotoxicity: Generation of reactive oxygen species", *Journal of Food and Drug Analysis*, 22(1), pp. 64–75, 2014.
<https://doi.org/10.1016/j.jfda.2014.01.005>
- [11] Gołębiewska, A., Kobylański, M. P., Zaleska-Medynska, A. "2 - Fundamentals of metal oxide-based photocatalysis", In: *Metal Oxide-Based Photocatalysis: Fundamentals and Prospects for Application*, Elsevier, 2018, pp. 3–50.
<https://doi.org/10.1016/B978-0-12-811634-0.00002-0>
- [12] Uma, S., Shobana, M. K. "Metal oxide semiconductor gas sensors in clinical diagnosis and environmental monitoring", *Sensors and Actuators A: Physical*, 349, 114044, 2023.
<https://doi.org/10.1016/j.sna.2022.114044>
- [13] He, H. "2 - Metal oxide semiconductors and conductors", In: *Cui, Z., Korotcenkov, G. (eds.) Solution Processed Metal Oxide Thin Films for Electronic Applications*, Elsevier, 2020, pp. 7–30.
<https://doi.org/10.1016/B978-0-12-814930-0.00002-5>
- [14] Opong, S. O. B., Opoku, F., Govender, P. P. "Tuning the electronic and structural properties of Gd-TiO₂-GO nanocomposites for enhancing photodegradation of IC dye: The role of Gd³⁺ ion", *Applied Catalysis B: Environmental*, 243, pp. 106–120, 2019.
<https://doi.org/10.1016/j.apcatb.2018.10.031>
- [15] Goodarzi, N., Ashrafi-Peyman, Z., Khani, E., Moshfegh, A. Z. "Recent Progress on Semiconductor Heterogeneous Photocatalysts in Clean Energy Production and Environmental Remediation", *Catalysts*, 13(7), 1102, 2023.
<https://doi.org/10.3390/catal13071102>
- [16] Bhuyan, A., Ahmaruzzaman, M. "Ultrasonic-assisted synthesis of highly efficient, robust metal oxide QDs immobilized-MOF-5/Ni-Co-LDH photocatalyst for sunlight-mediated degradation of multiple toxic dyes", *Journal of Alloys and Compounds*, 972, 172781, 2024.
<https://doi.org/10.1016/j.jallcom.2023.172781>
- [17] Andish-Lifshagerd, F., Habibi-Yangjeh, A., Habibi, M., Akinay, Y. "Facile synthesis of ZnO/CeO₂/CeFeO₃ photocatalysts sensitive to visible light with tandem n-n heterojunctions and improved performance towards tetracycline and dye effluent removals", *Journal of Photochemistry and Photobiology A: Chemistry*, 448, 115351, 2024.
<https://doi.org/10.1016/j.jphotochem.2023.115351>
- [18] Yik, C., Yao, J., Sze, L., Yi, P., Hong, Z. "Visible light-driven dye degradation by magnetic cobalt-doped zinc oxide / iron oxide photocatalyst", *Next Materials*, 2, 100074, 2024.
<https://doi.org/10.1016/j.nxmate.2023.100074>

- [19] Rianjanu, A., Mustamin, A. S. P., Melati, E. K. A., Aflaha, R., Khamidy, N. I., ... Taher, T. "Photocatalytic degradation of aqueous Congo red dye pollutants by rare-earth metal oxide (CeO₂) nanorods", *Colloids and Surfaces A: Physicochemical and Engineering Aspects*, 682, 132919, 2024.
<https://doi.org/10.1016/j.colsurfa.2023.132919>
- [20] Hernández-Del Castillo, P. C., Robledo-Trujillo, G., Rodríguez-González, V. "Development of a visible-light-active-NiTiO₃ coating for the efficient removal of the persistent herbicide 2,6-dichlorobenzamide (BAM) from drinking water", *Chemosphere*, 339, 2024.
<https://doi.org/10.1016/j.chemosphere.2023.139628>
- [21] Kocijan, M., Ćurković, L., Vengust, D., Radošević, T., Shvalya, V., Gonçalves, G., Podlogar, M. "Synergistic Remediation of Organic Dye by Titanium Dioxide/Reduced Graphene Oxide Nanocomposite", *Molecules*, 28(21), 7326, 2023.
<https://doi.org/10.3390/molecules28217326>
- [22] Bezu, Z., Taddesse, A. M., Diaz, I. "Natural zeolite supported g-C₃N₄/ZnO/Ag₃PO₄ composite: A tandem n-n heterojunction for simultaneous photodegradation of dyes under visible and solar irradiation", *Journal of Photochemistry and Photobiology A: Chemistry*, 449, 115369, 2024.
<https://doi.org/10.1016/j.jphotochem.2023.115369>
- [23] Subalakshmi, A., Kavitha, B., Srinivasan, N., Rajarajan, M., Suganthi, A. "Evaluation of photocatalytic activity of Cu₃(PO₄)₂/MgO nanocomposite for the efficient removal of amaranth dye under solar light irradiation", *Inorganic Chemistry Communications*, 161, 112033, 2024.
<https://doi.org/10.1016/j.inoche.2024.112033>
- [24] Gupta, A., Kajal, Ajravat, K., Brar, L. K., Pandey, O. P., Rajagopalan, P. "Facile synthesis of Mn₃O₄-ZnO composite for photocatalytic dye removal and capacitive applications", *Materials Chemistry and Physics*, 313, 128698, 2024.
<https://doi.org/10.1016/j.matchemphys.2023.128698>
- [25] Barakat, N. A. M., Omran, H. A., Hassan, M. K., Mohamed, A. F., Backar, A. H., Irfan, O. M., Mohamed, O. A. "Graphite-TiO₂-doped coated sand granules for efficient continuous removal of methylene blue dye: Combining adsorption and photocatalytic degradation", *Results in Engineering*, 20, 101646, 2023.
<https://doi.org/10.1016/j.rineng.2023.101646>
- [26] Pouthika, K., Madhumitha, G. "Design and development of Carissa edulis fruit extract mediated bimetallic CuO-NiO-HNT composites for photocatalytic removal of food dye and antibiotic drug", *Journal of Molecular Structure*, 1295, 136665, 2024.
<https://doi.org/10.1016/j.molstruc.2023.136665>
- [27] Bólla de Menezes, L., Muraro, P. C. L., Druzian, D. M., Ruiz, Y. P. M., Galembeck, A., Pavoski, G., Espinosa, D. C. R., da Silva, W. L. "Calcium oxide nanoparticles: Biosynthesis, characterization and photocatalytic activity for application in yellow tartrazine dye removal", *Journal of Photochemistry and Photobiology A: Chemistry*, 447, 115182, 2024.
<https://doi.org/10.1016/j.jphotochem.2023.115182>
- [28] Yu, Y., Kuang, X., Jin, X., Chen, F., Min, J., Duan, H., Li, J., Wu, Z., Cao, B. "Synergistic effect of oxygen vacancies and doped sulfur over BiOBr for efficient visible photocatalytic removal of dyes", *Applied Surface Science*, 649, 159169, 2024.
<https://doi.org/10.1016/j.apsusc.2023.159169>
- [29] Pham, V. V., Ngoc, T., Nguyen, U., Khanh, C., Khoa, T. "Efficient visible-light-driven photocatalytic performance for nitrogen oxide abatement application in the air by a typical metal / semiconductor heterojunction", *Chemical Physics Letters*, 835, 141017, 2024.
<https://doi.org/10.1016/j.cplett.2023.141017>
- [30] Grabchenko, M. V., Mamontov, G. V., Chernykh, M. V., Vodyankina, O. V., Salaev, M. A. "Synergistic effect in ternary CeO₂-ZrO₂-MnO_x catalysts for CO oxidation and soot combustion", *Chemical Engineering Science*, 285, 119593, 2024.
<https://doi.org/10.1016/j.ces.2023.119593>
- [31] Patrick, D. S., Bharathi, P., Kamalakannan, S., Archana, J., Navaneethan, M., Krishna Mohan, M. "Confined oxidation of 2D WS₂ nanosheets forming WO₃/WS₂ nanocomposites for room temperature NO₂ gas sensing application", *Applied Surface Science*, 642, pp. 158554, 2024.
<https://doi.org/10.1016/j.apsusc.2023.158554>
- [32] Jamnani, S. R., Moghaddam, H. M., Leonardi, S. G., Neri, G., Ferlazzo, A. "VOCs sensing properties of samarium oxide nanorods", *Ceramics International*, 50(1), pp. 403–411, 2024.
<https://doi.org/10.1016/j.ceramint.2023.10.115>
- [33] Nguyen, H. P., Cao, T. M., Nguyen, T. T., Pham, V. V. "Improving photocatalytic oxidation of semiconductor (TiO₂, SnO₂, ZnO)/CNTs for NO_x removal", *Journal of Industrial and Engineering Chemistry*, 127, pp. 321–330, 2023.
<https://doi.org/10.1016/j.jiec.2023.07.017>
- [34] Tamura, T., Ohyama, J., Sawabe, K., Satsuma, A. "Enhanced CO oxidation by reversible structural variation of supported Ag nanoparticle catalyst from single to twin by CO treatment", *Catalysis Today*, 411–412, 113814, 2023.
<https://doi.org/10.1016/j.cattod.2022.06.029>
- [35] Busch, M., Kompch, A., Suleiman, S., Notthoff, C., Bergmann, U., Theissmann, R., Atakan, B., Winterer, M. "NO_x conversion properties of a novel material: Iron nanoparticles stabilized in carbon", *Applied Catalysis B: Environmental*, 166–167, pp. 211–216, 2015.
<https://doi.org/10.1016/j.apcatb.2014.11.013>
- [36] Li, S., Zheng, Z., Zhao, Z., Wang, Y., Yao, Y., Liu, Y., Zhang, J., Zhang, Z. "CeO₂ Nanoparticle-Loaded MnO₂ Nanoflowers for Selective Catalytic Reduction of NO_x with NH₃ at Low Temperatures", *Molecules*, 27(15), 4863, 2022.
<https://doi.org/10.3390/molecules27154863>
- [37] Soubaihi, R. M. A., Saoud, K. M., Dutta, J. "Low-temperature CO oxidation by silver nanoparticles in silica aerogel mesoreactors", *Chemical Engineering Journal*, 455, 140576, 2023.
<https://doi.org/10.1016/j.cej.2022.140576>
- [38] Altass, H. M., Ahmed, S. A., Salama, R. S., Moussa, Z., Jassas, R. S., ... Khder, A. S. "Low Temperature CO Oxidation Over Highly Active Gold Nanoparticles Supported on Reduced Graphene Oxide@Mg-BTC Nanocomposite", *Catalysis Letters*, 153(3), pp. 876–886, 2023.
<https://doi.org/10.1007/s10562-022-04026-y>
- [39] Camposeco, R., Castillo, S., Hinojosa-Reyes, M., Nava, N., Zanella, R. "Efficient CO (carbon monoxide) oxidation using gold catalysts supported on WO₃ /titanate protonated nanotubes", *Materials Research Bulletin*, 115, pp. 247–256, 2019.
<https://doi.org/10.1016/j.materresbull.2019.04.004>

- [40] Kim, I. H., Seo, H. O., Park, E. J., Han, S. W., Kim, Y. D. "Low Temperature CO oxidation over Iron Oxide Nanoparticles Decorating Internal Structures of a Mesoporous Alumina", *Scientific Reports*, 7, 40497, 2017.
<https://doi.org/10.1038/srep40497>
- [41] Liu, T., Zheng, M., Hao, P., Ji, K., Shao, M., Duan, H. "Efficient photo-oxidation remediation strategy toward arsenite-contaminated water and soil with zinc-iron layered double hydroxide as amendment", *Journal of Environmental Chemical Engineering*, 11(1), 109233, 2023.
<https://doi.org/10.1016/j.jece.2022.109233>
- [42] Deng, H., Lei, H., Luo, Y., Huan, C., Li, J., Li, H., He, F., Zhang, B., Yi, K., Sun, A. "The effects of titanium dioxide nanoparticles on cadmium bioaccumulation in ramie and its application in remediation of cadmium-contaminated soil", *Alexandria Engineering Journal*, 86, pp. 663–668, 2024.
<https://doi.org/10.1016/j.aej.2023.12.019>
- [43] Ghafghazi, L., Taghavi, L., Rasekh, B., Farahani, H., Hassani, A. H. "Application of compost assisted by Fe₃O₄ nanoparticles in di (2-ethylhexyl) phthalate-contaminated soil remediation: Biostimulation strategy, Soil responses, and RSM/CCD Optimization", *Science of the Total Environment*, 908, 168029, 2024.
<https://doi.org/10.1016/j.scitotenv.2023.168029>
- [44] Chakravarty, P., Deka, H., Chowdhury, D. "Anthracene removal potential of green synthesized titanium dioxide nanoparticles (TiO₂-NPs) and *Alcaligenes faecalis* HP8 from contaminated soil", *Chemosphere*, 321, 138102, 2023.
<https://doi.org/10.1016/j.chemosphere.2023.138102>
- [45] Barzegar, G., Jorfi, S., Soltani, R. D. C., Ahmadi, M., Saeedi, R., Abtahi, M., Ramavandi, B., Baboli, Z. "Enhanced Sono-Fenton-Like Oxidation of PAH-Contaminated Soil Using Nano-Sized Magnetite as Catalyst: Optimization with Response Surface Methodology", *Soil and Sediment Contamination*, 26(5), pp. 538–557, 2017.
<https://doi.org/10.1080/15320383.2017.1363157>
- [46] Bakshi, M., Kumar, A. "Co-application of TiO₂ nanoparticles and hyperaccumulator *Brassica juncea* L. for effective Cd removal from soil: Assessing the feasibility of using nano-phytoremediation", *Journal of Environmental Management*, 341, 118005, 2023.
<https://doi.org/10.1016/j.jenvman.2023.118005>
- [47] Pérez-Hernández, H., Pérez-Moreno, A. Y., Méndez-López, A., Fernández-Luqueño, F. "Effect of ZnO Nanoparticles During the Process of Phytoremediation of Soil Contaminated with As and Pb Cultivated with Sunflower (*Helianthus annuus* L.)", *International Journal of Environmental Research*, 18(1), 7, 2024.
<https://doi.org/10.1007/s41742-023-00556-4>
- [48] Kuang, X., Shao, J., Peng, L., Song, H., Wei, X., Luo, S., Gu, J.-D. "Nano-TiO₂ enhances the adsorption of Cd(II) on biological soil crusts under mildly acidic conditions", *Journal of Contaminant Hydrology*, 229, 103583, 2020.
<https://doi.org/10.1016/j.jconhyd.2019.103583>
- [49] Singh, A., Chaudhary, S., Dehiya, B. S. "Fast removal of heavy metals from water and soil samples using magnetic Fe₃O₄ nanoparticles", *Environmental Science and Pollution Research*, 28(4), pp. 3942–3952, 2021.
<https://doi.org/10.1007/s11356-020-10737-9>
- [50] Wang, A.-N., Teng, Y., Hu, X.-F., Wu, L.-H., Huang, Y.-J., Luo, Y.-M., Christie, P. "Diphenylarsinic acid contaminated soil remediation by titanium dioxide (P25) photocatalysis: Degradation pathway, optimization of operating parameters and effects of soil properties", *Science of the Total Environment*, 541, pp. 348–355, 2016.
<https://doi.org/10.1016/j.scitotenv.2015.09.023>
- [51] Duncan, E., Owens, G. "Metal oxide nanomaterials used to remediate heavy metal contaminated soils have strong effects on nutrient and trace element phytoavailability", *Science of the Total Environment*, 678, pp. 430–437, 2019.
<https://doi.org/10.1016/j.scitotenv.2019.04.442>
- [52] Lan, Y., Lu, Y., Ren, Z. "Mini review on photocatalysis of titanium dioxide nanoparticles and their solar applications", *Nano Energy*, 2(5), pp. 1031–1045, 2013.
<https://doi.org/10.1016/j.nanoen.2013.04.002>
- [53] Ruiz-Santoyo, V., Marañón-Ruiz, V., Romero-Toledo, R., Vargas, O. G., Pérez-Larios, A. "Photocatalytic Degradation of Rhodamine B and Methylene Orange Using TiO₂-ZrO₂ as Nanocomposite", *Catalysts*, 11(9), 1035, 2021.
<https://doi.org/10.3390/catal11091035>
- [54] Zahmatkesh, S., Hajiaghahi-Keshteli, M., Bokhari, A., Sundaramurthy, S., Panneerselvam, B., Rezakhani, Y. "Wastewater treatment with nanomaterials for the future: A state-of-the-art review", *Environmental Research*, 216, 114652, 2023.
<https://doi.org/10.1016/j.envres.2022.114652>
- [55] Wang, Y., Zhao, S., Yang, Y., Rodriguez, R. D., Lipovka, A., Lu, Y., Huang, H., Chen, J. "Ag nanoparticle-decorated Bi₂O₃-TiO₂ heterogeneous nanotubular photocatalysts for enhanced degradation of organic contaminants", *Colloids and Surfaces A: Physicochemical and Engineering Aspects*, 648, 129233, 2022.
<https://doi.org/10.1016/j.colsurfa.2022.129233>
- [56] Boretti, A., Rosa, L. "Reassessing the projections of the World Water Development Report", *npj Clean Water*, 2, 15, 2019.
<https://doi.org/10.1038/s41545-019-0039-9>
- [57] Rayaroth, M. P., Aravindakumar, C. T., Shah, N. S., Boczkaj, G. "Advanced oxidation processes (AOPs) based wastewater treatment - unexpected nitration side reactions - a serious environmental issue: A review", *Chemical Engineering Journal*, 430, 133002, 2022.
<https://doi.org/10.1016/j.cej.2021.133002>
- [58] Şimşek, B., Sevgili, I., Ceran, Ö. B., Korucu, H., Şara, O. N. "Nanomaterials based drinking water purification: Comparative study with a conventional water purification process", *Periodica Polytechnica Chemical Engineering*, 63(1), pp. 96–112, 2019.
<https://doi.org/10.3311/PPCh.12458>
- [59] Fuller, R., Landrigan, P. J., Balakrishnan, K., Bathan, G., Bose-O'Reilly, S., ... Yan, C. "Pollution and health: a progress update", *The Lancet Planetary Health*, 6(6), pp. e535–e547, 2022.
[https://doi.org/10.1016/S2542-5196\(22\)00090-0](https://doi.org/10.1016/S2542-5196(22)00090-0)
- [60] Tran, H. M., Tsai, F.-J., Lee, Y.-L., Chang, J.-H., Chang, L.-T., ... Chuang, H.-C. "The impact of air pollution on respiratory diseases in an era of climate change: A review of the current evidence", *Science of the Total Environment*, 898, 166340, 2023.
<https://doi.org/10.1016/j.scitotenv.2023.166340>

- [61] Zhu, B. Zhang, L. Y., Li, M., Yan, Y., Zhang, X. M., Zhu, Y. M. "High-performance of plasma-catalysis hybrid system for toluene removal in air using supported Au nanocatalysts", *Chemical Engineering Journal*, 381, 122599, 2020.
<https://doi.org/10.1016/j.cej.2019.122599>
- [62] An, D., Wang, Y., Dai, J., Guo, L., Liu, N. "Synthesis of Pr doped In_2O_3 nanoparticles and their enhanced ethanol gas-sensing performance", *Ceramics International*, 50(3), pp. 4945–4954, 2024.
<https://doi.org/10.1016/j.ceramint.2023.11.237>
- [63] Wuepper, D., Borrelli, P., Finger, R. "Countries and the global rate of soil erosion", *Nature Sustainability*, 3, pp. 51–55, 2020.
<https://doi.org/10.1038/s41893-019-0438-4>
- [64] Borrelli, P., Robinson, D. A., Fleischer, L. R., Lugato, E., Ballabio, C., ... Panagos, P. "An assessment of the global impact of 21st century land use change on soil erosion", *Nature Communications*, 8, 2013, 2017.
<https://doi.org/10.1038/s41467-017-02142-7>
- [65] Thakur, N., Thakur, N., Kumar, A., Kumar Thakur, V., Kalia, S., Arya, V., Kumar, A., Kumar, S., Kyzas, G. Z. "A critical review on the recent trends of photocatalytic, antibacterial, antioxidant and nanohybrid applications of anatase and rutile TiO_2 nanoparticles", *Science of The Total Environment*, 914, 169815, 2024.
<https://doi.org/10.1016/j.scitotenv.2023.169815>